



# ME-446: Liquid-gas interfacial heat and mass transfer

## Boiling III

Zhengmao Lu  
Energy Transport Advances  
Laboratory  
EPFL Mechanical Engineering

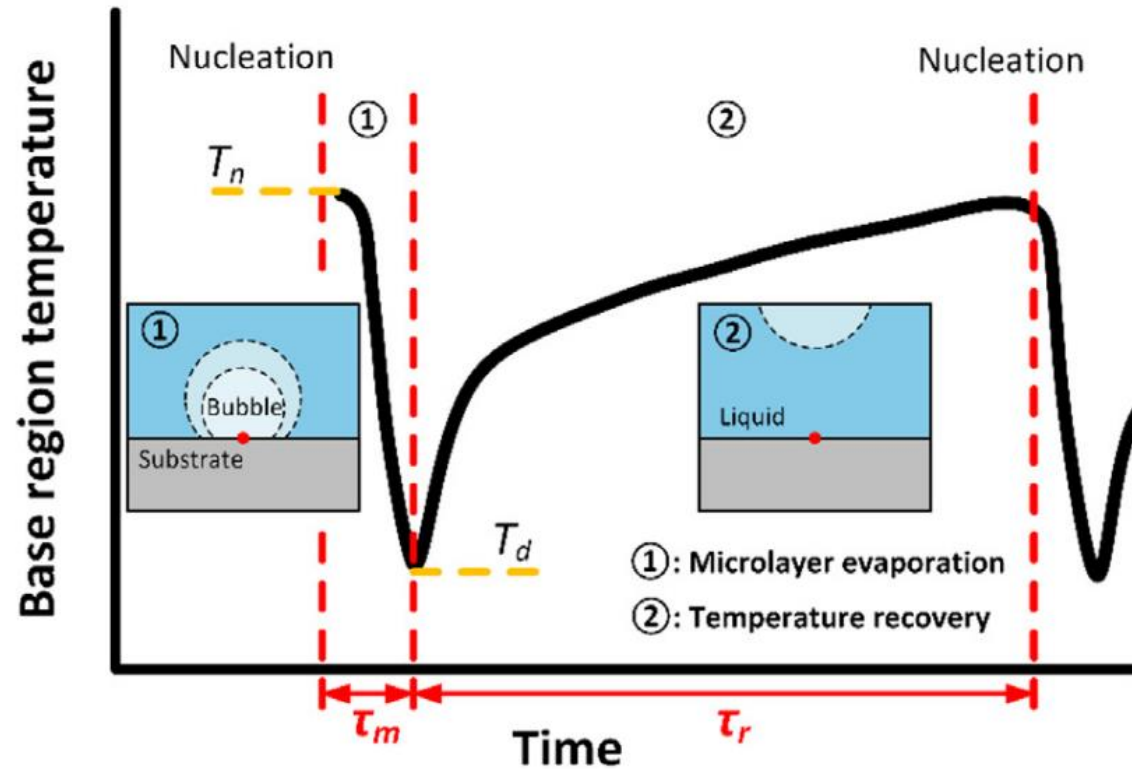
2024 Fall Semester

Photo Credit: Trougnouf

- Entrapped gas/vapor theory
- Onset of nucleation coupled with thermal boundary layer (Hsu's model)

# Intended Learning Objectives Today

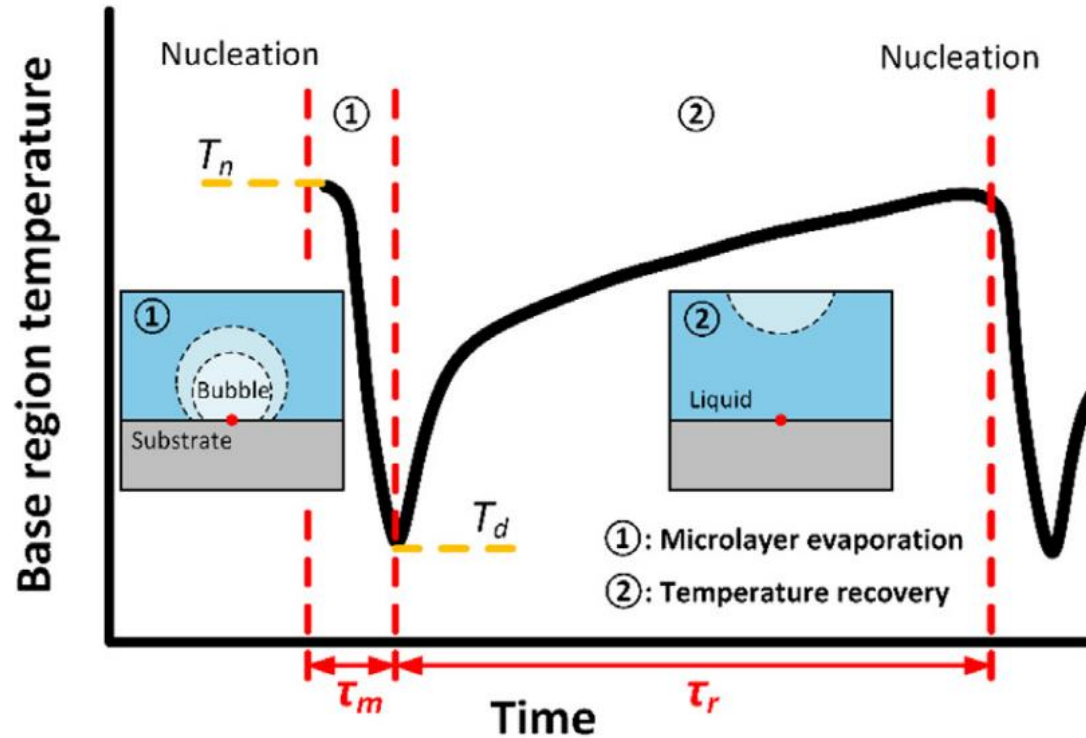
- Bubble departure frequency and diameter
- Different regimes in pool boiling
- Rohsenow's microconvection model for nucleate boiling
- Zuber's CHF model based on Helmholtz and Taylor instabilities



- Right after nucleation, substrate temperature drops due to rapid evaporation
- After bubble departure, the substrate needs to be reheated through convection and conduction to reach nucleation temperature again

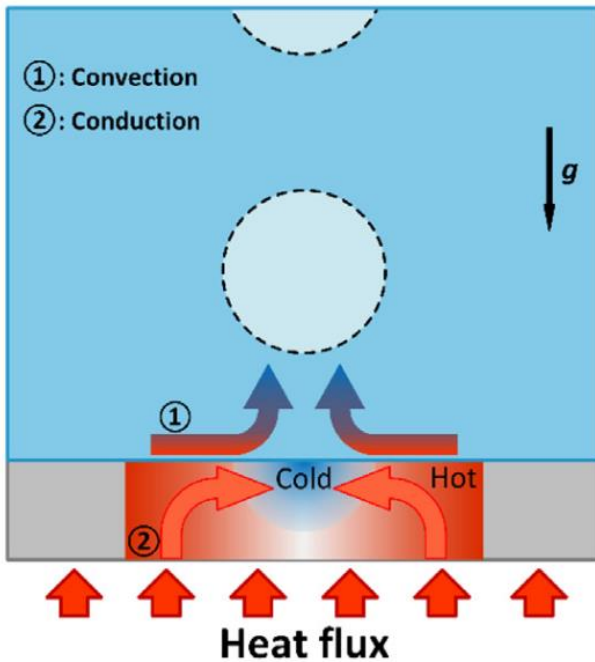
Zhang *et al.*, 2021

<https://doi.org/10.1016/j.ijheatmasstransfer.2020.120640>

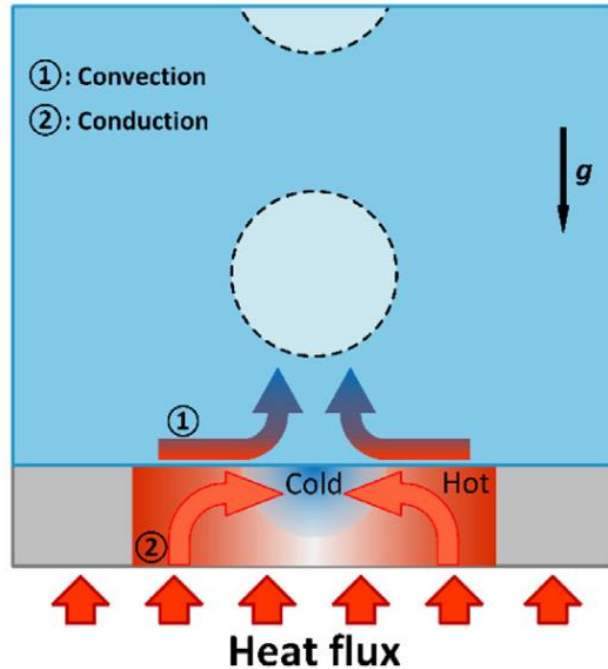


We are interested in departure frequency and the departure bubble size

In isolated bubble regime, evaporation (cooling) much faster than temperature recovery (heating)

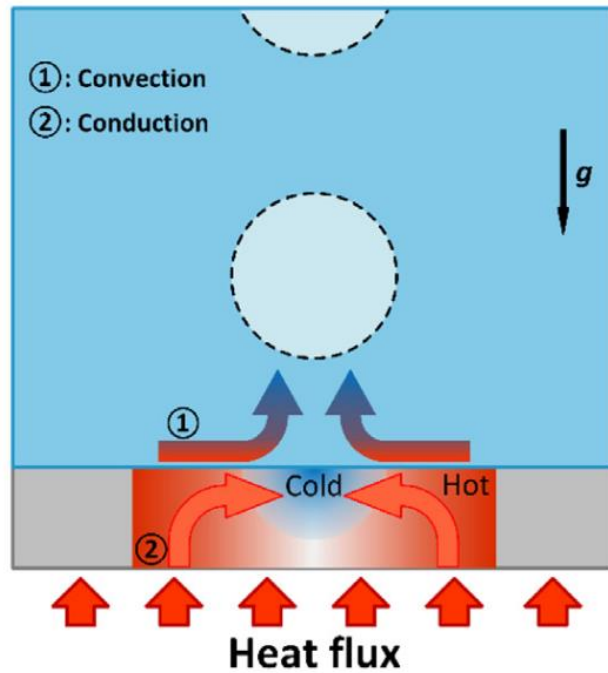


- ① Rewetting of surrounding superheated liquid
- ② Heat conduction from surrounding solid region



## ① Rewetting of surrounding superheated liquid

Transient heat conduction of a semi-infinite wall with a convective boundary condition

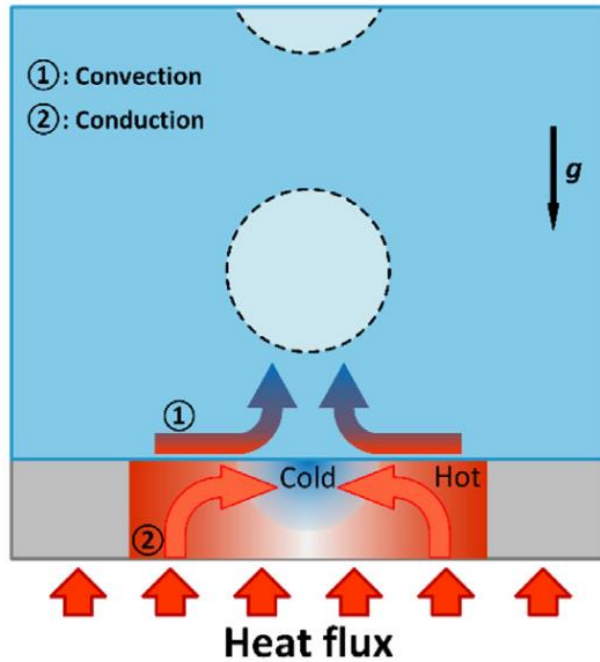


- ① Rewetting of surrounding superheated liquid

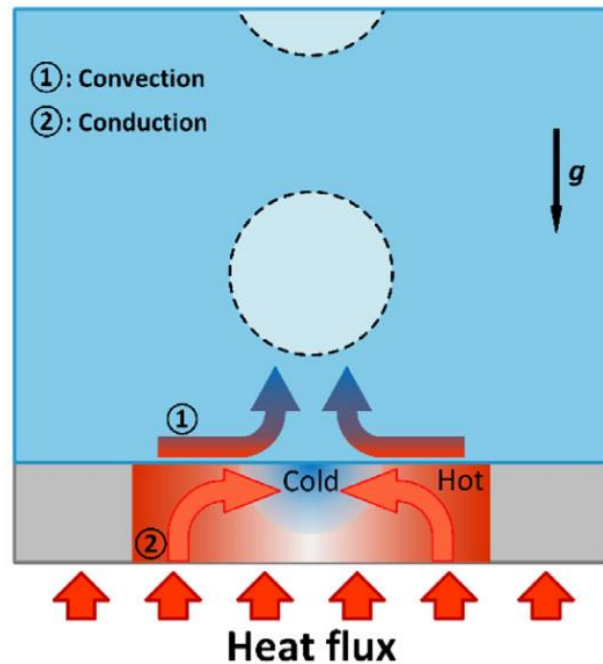
$$\tau_w = \frac{k_s^2}{h^2 \alpha_s}$$

How to determine  $h$





② Heat conduction from surrounding solid region

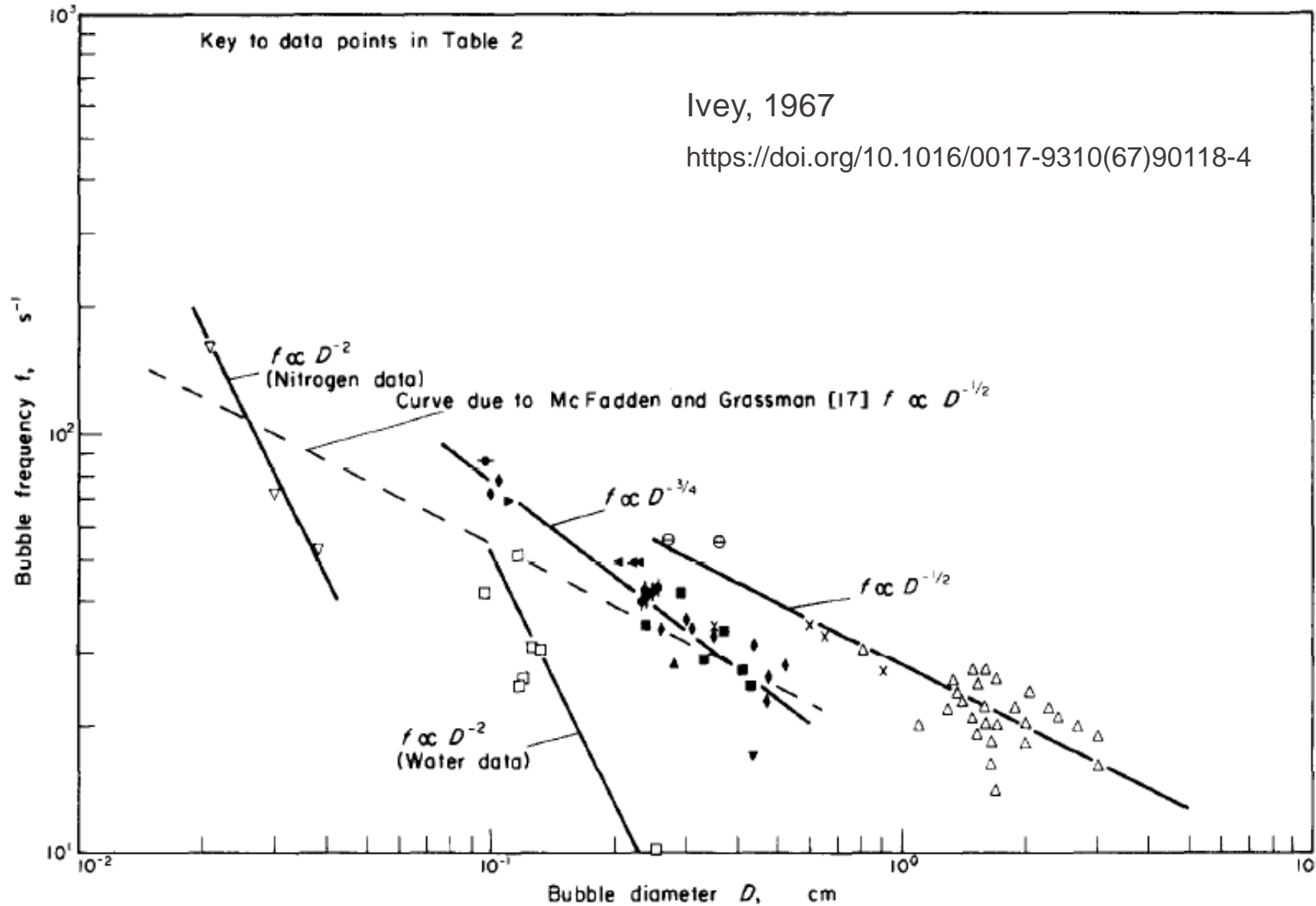


- Rewetting and heat conduction are two competing mechanisms for temperature recovery

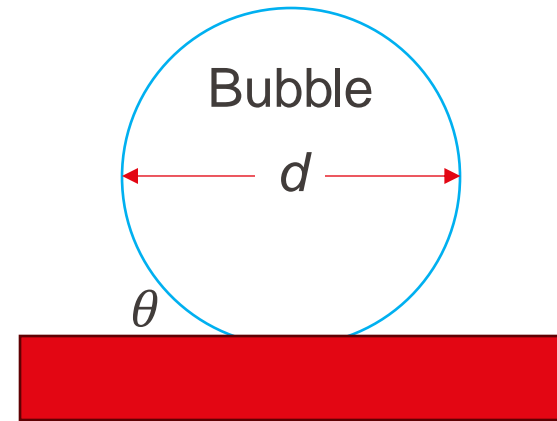
$$\frac{\tau_d}{\tau_w} \sim D^{1.5}$$

When  $D$  is relatively large, rewetting-induced convection dominates

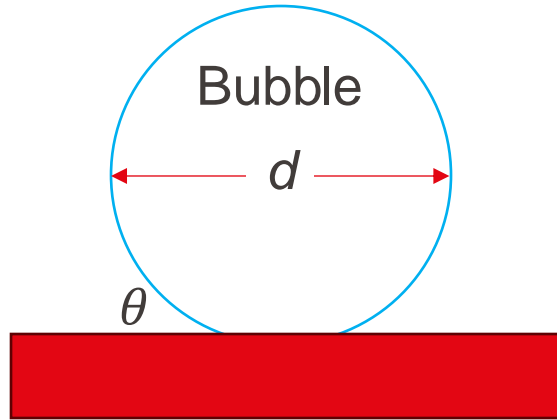
When  $D$  is relatively small, conduction dominates



# Bubble Departure Diameter



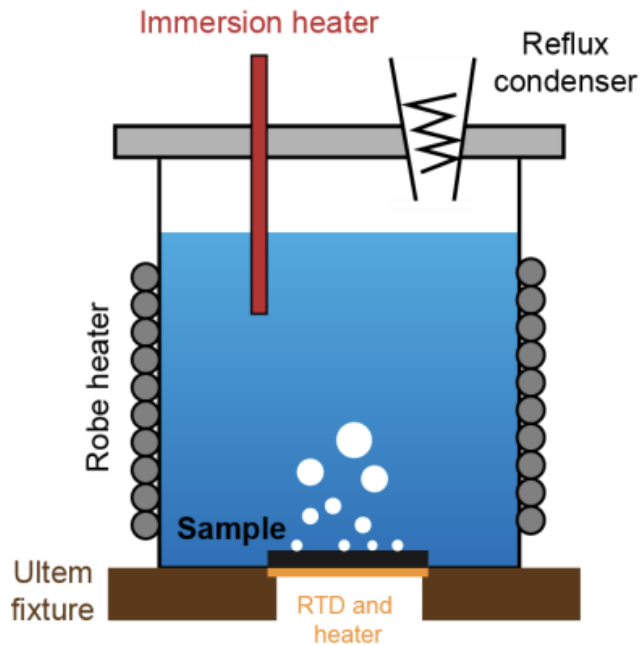
# Comments on Fritz's Expression



Simple balance between surface tension force and buoyancy force. The effect of the contact angle is taken into account in an empirical manner

At different heat fluxes, the bubble may have different growth rate, corresponding to a different momentum force

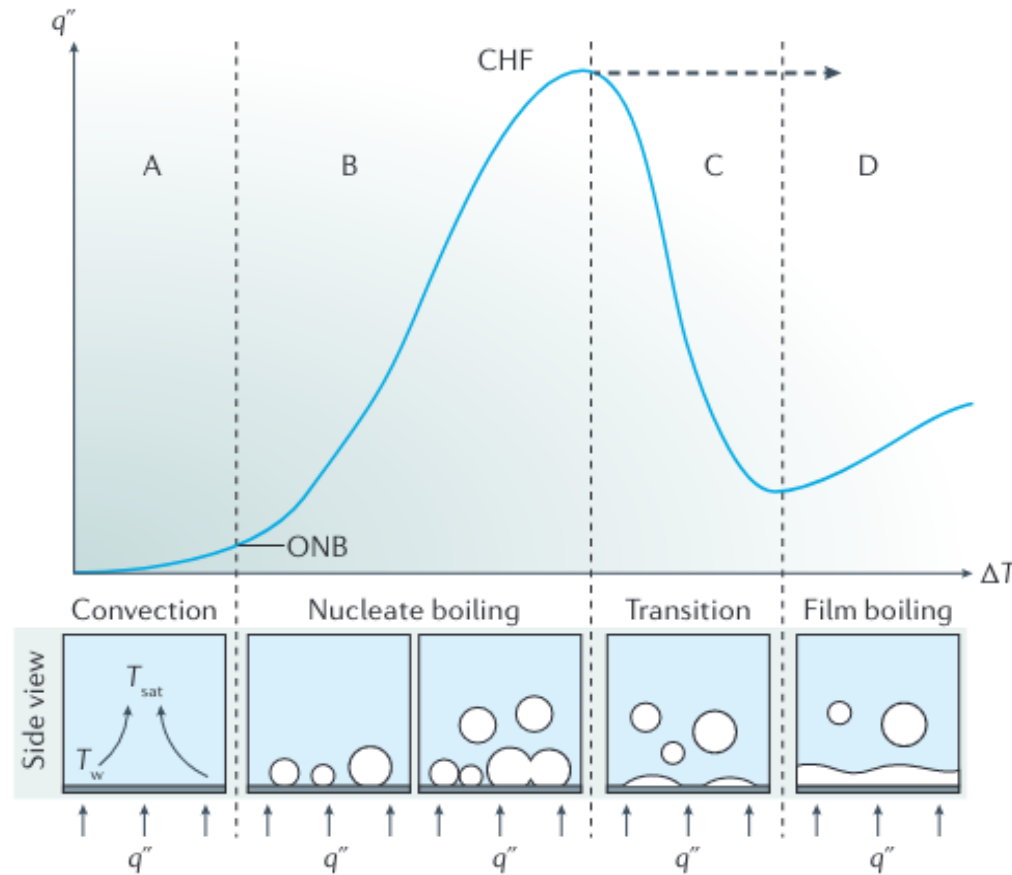
Archimedes' principles not exactly suitable given that there is no liquid underneath the bubble base



Capillary length  $L_b = \sqrt{\frac{\sigma}{g(\rho_l - \rho_v)}}$  by setting  $Bo = 1$

Pool boiling surface characteristic length  $L \gg L_b$

We are interested in the relationship between the average heat flux at the boiling surface  $q''$  and the surface super heat  $\Delta T = T_w - T_{sat}(P_l)$



A. At very low superheats, heat transfer is mostly due to natural convection

B. After superheat is large enough to form vapor bubbles, nucleate boiling dominates, promoting bubble-motion-induced convection

C-D. After vapor generation becomes too much, passing the critical heat flux (CHF), insulating vapor film will start to form, decreasing the HTC

Convective transport facilitated by bubbles

$$\text{Nu}_b = \frac{hL_b}{k_l} \propto \text{Re}_b^{1-r} \text{Pr}_l^{1-s}$$

$$\text{Re}_b = \frac{\rho_v U L_b}{\mu_L} \quad U = \frac{q''}{\rho_v h_{lv}} = \frac{h \Delta T}{\rho_v h_{lv}}$$

$$\frac{q''}{\mu_l h_{lv}} \left[ \frac{\sigma}{g(\rho_l - \rho_v)} \right]^{1/2} = \left( \frac{1}{C_{sf}} \right)^{1/r} \text{Pr}_l^{-s/r} \left[ \frac{c_{pl} \Delta T}{h_{lv}} \right]^{1/r}$$



# Rohsenow's Microconvection Model

$$\frac{q''}{\mu_l h_{lv}} \left[ \frac{\sigma}{g(\rho_l - \rho_v)} \right]^{1/2} = \left( \frac{1}{C_{sf}} \right)^{1/r} \text{Pr}_l^{-s/r} \left[ \frac{c_{pl} \Delta T}{h_{lv}} \right]^{1/r}$$

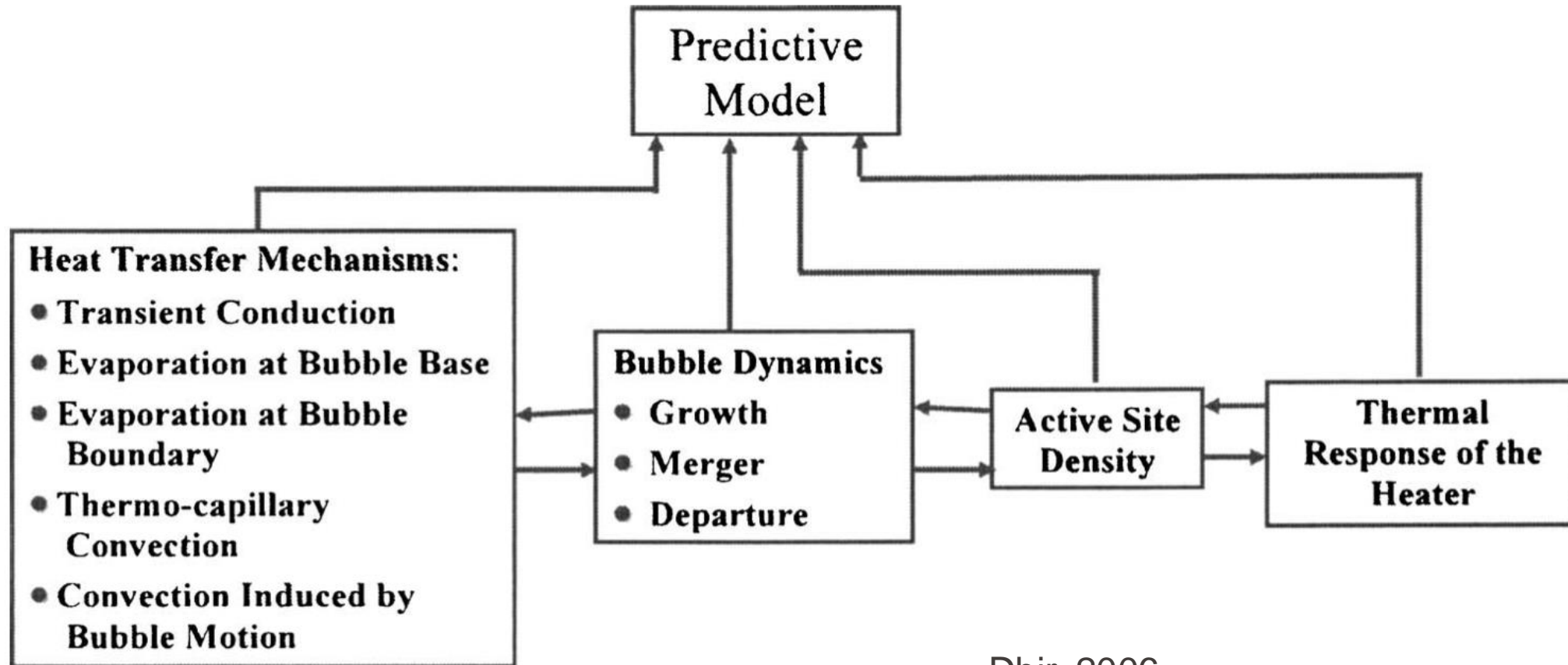
See Chapter 7.7 in Carey for recommended values of  $r$ ,  $s$ ,  $C_{sf}$

Most commonly used correlation for nucleate boiling heat transfer

For hydrophobic surfaces,  $C_{sf}$  is smaller.

Trapping gas/vapor is easier  $\Rightarrow$  More active bubble nucleation sites

# What's Needed for Mechanistic Understanding



Dhir, 2006

<https://doi.org/10.1115/1.2136366>

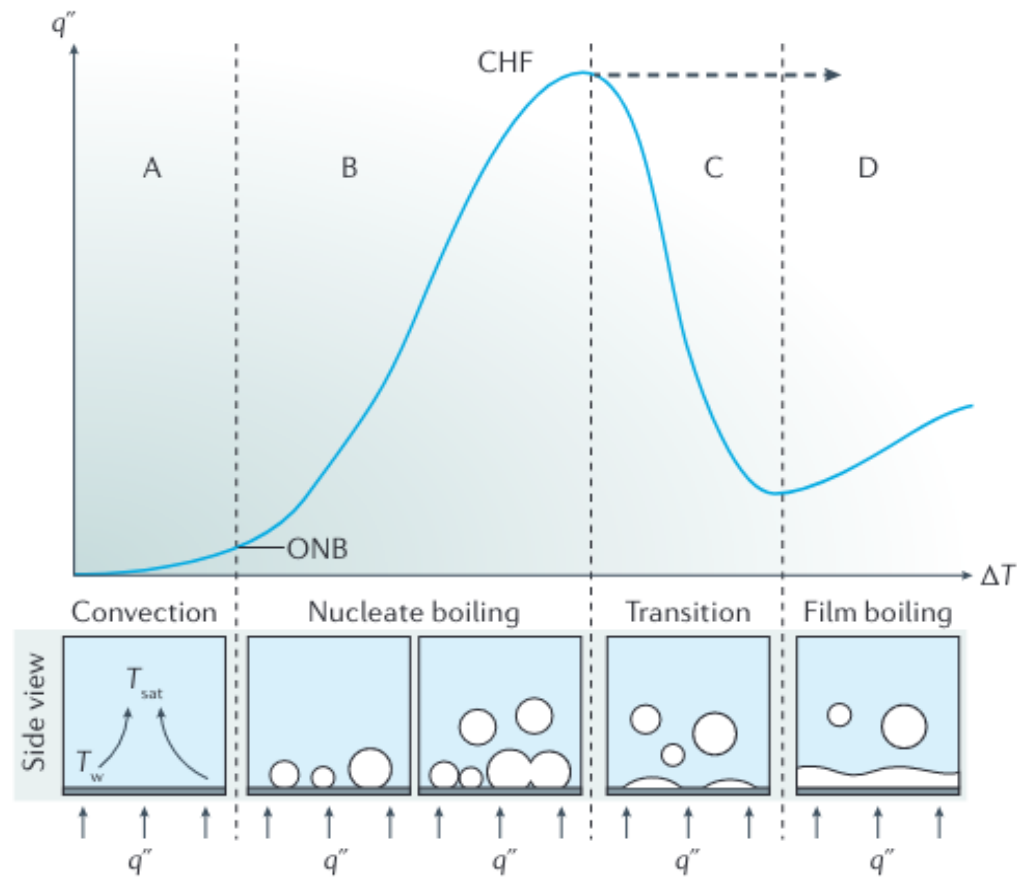


Working fluid: R134a

Heat flux:  
from 1.5 W/cm<sup>2</sup> to 38 W/cm<sup>2</sup>

Yazdani, 2016

<https://doi.org/10.1063/1.4940042>



U.S. Department of Energy  
Test of Nuclear Rods

# Helmholtz Instability of Vapor Columns

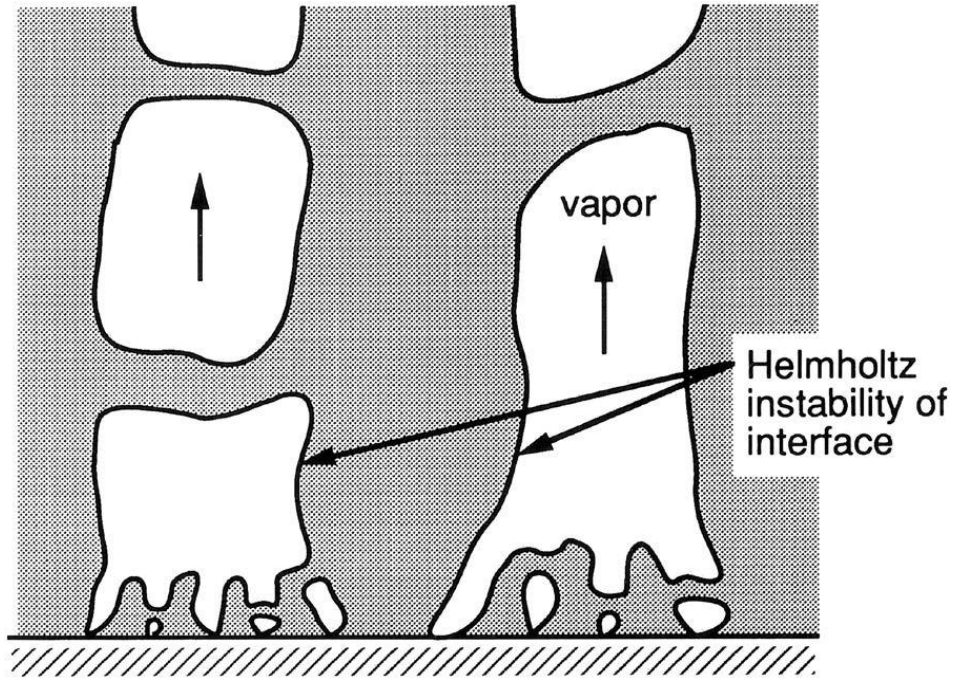
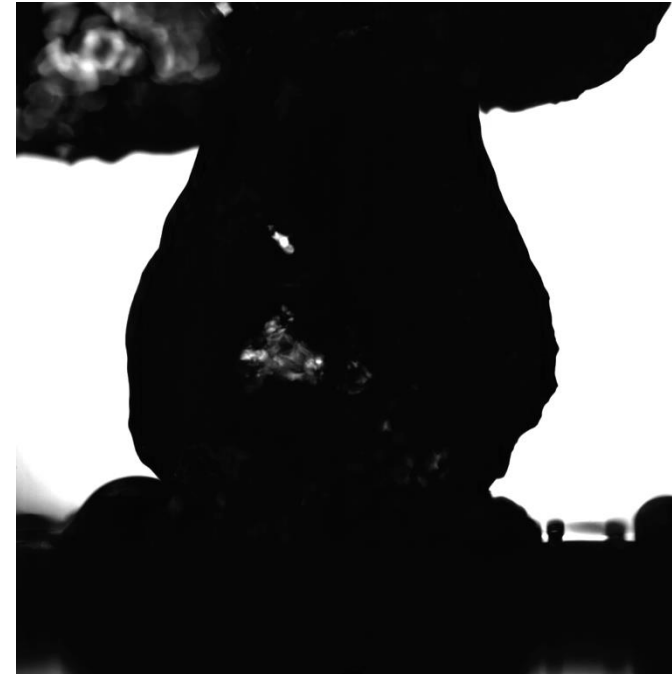


Figure 7.16 Carey



Video credit: Dr. Rameez Iqbal

Vapor columns form at high heat fluxes

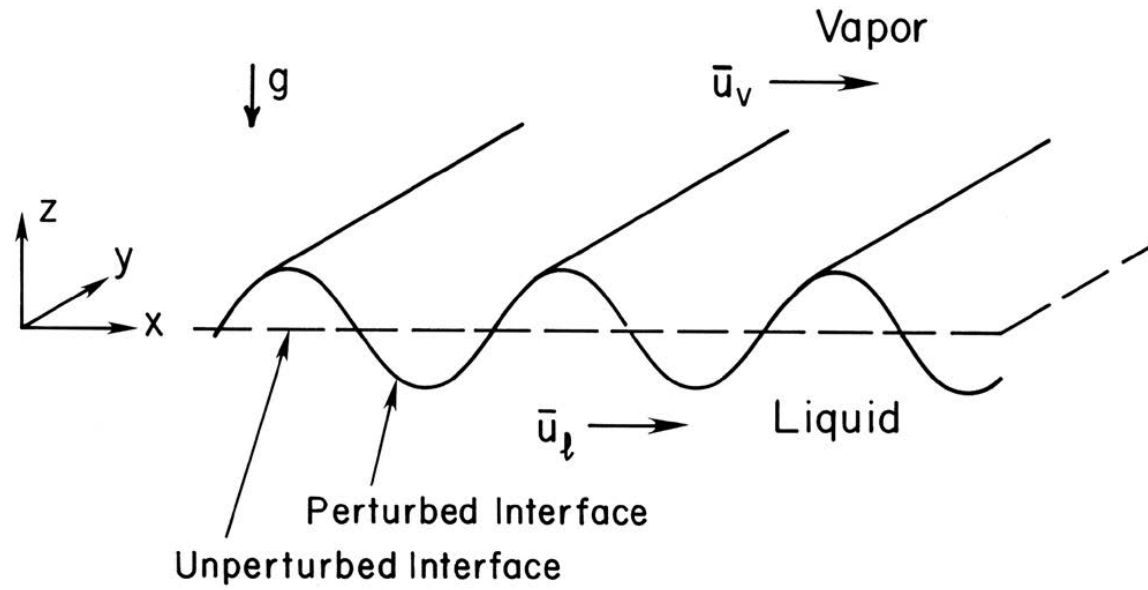
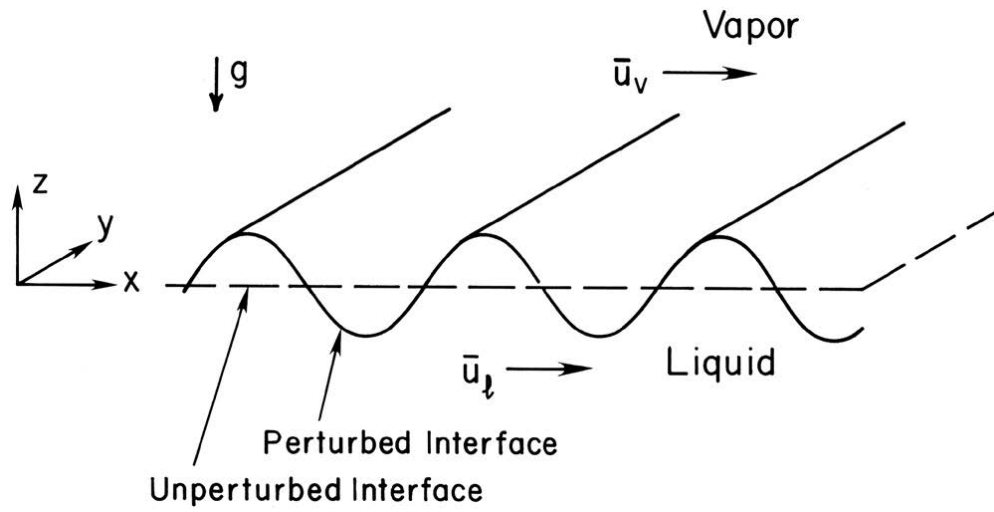


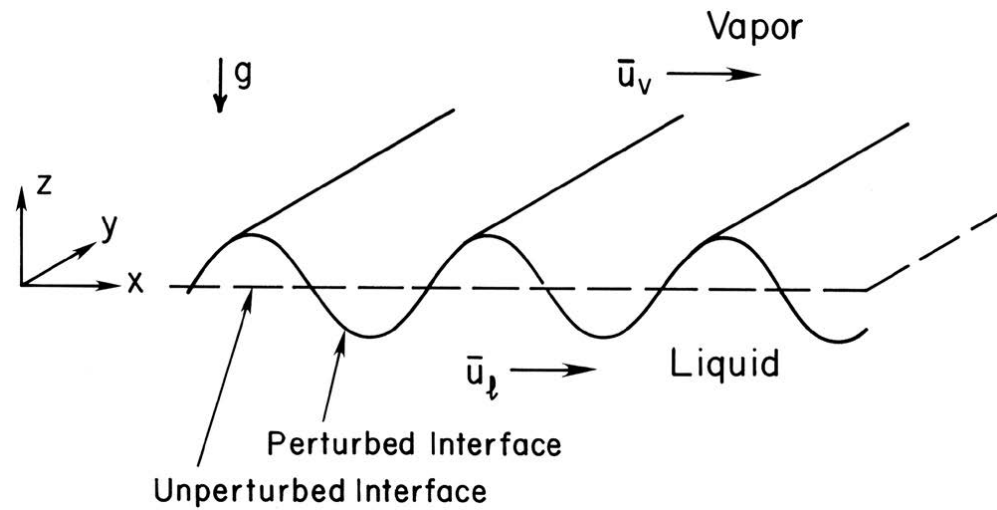
Figure 4.4 in Carey

# Helmholtz Instability



# Helmholtz Instability

$$\frac{\partial^2 P'}{\partial x^2} + \frac{\partial^2 P'}{\partial z^2} = 0 \quad P' = \hat{P}(z)e^{i\alpha x + \beta t}$$

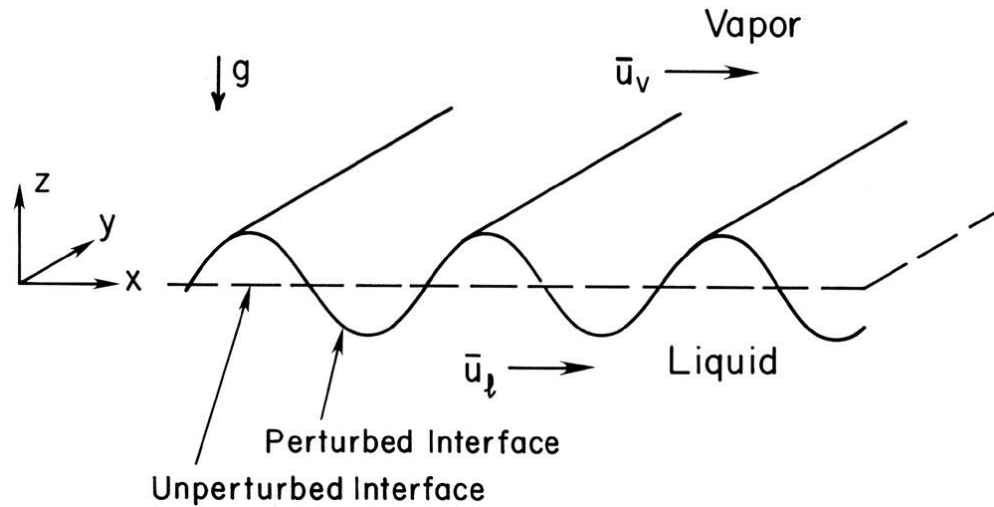


$$w' = \hat{w}(z)e^{i\alpha x + \beta t} \quad \rho \left( \frac{\partial w'}{\partial t} + \bar{u} \frac{\partial w'}{\partial x} \right) = - \frac{\partial P'}{\partial z}$$



# Helmholtz Instability

$$\frac{\partial u'}{\partial x} + \frac{\partial w'}{\partial z} = 0 \quad w' = \hat{w}(z)e^{i\alpha x + \beta t}$$



$$\delta = Ae^{i\alpha x + \beta t} \quad \hat{w}_v(z) = \frac{a_v \alpha}{\rho_v (\beta + i\alpha \bar{u})} e^{-\alpha z}$$

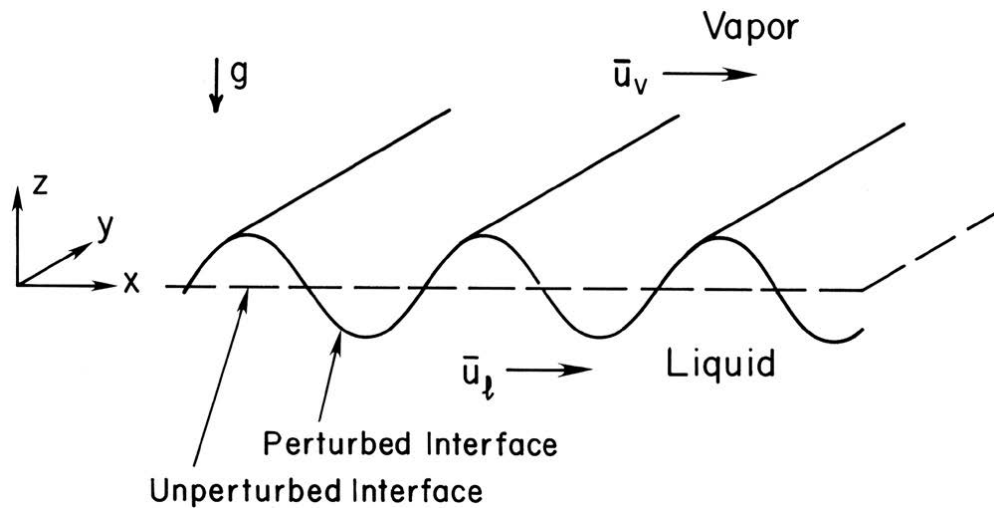
$$\hat{w}_l(z) = -\frac{a_l \alpha}{\rho_l (\beta + i\alpha \bar{u})} e^{\alpha z}$$

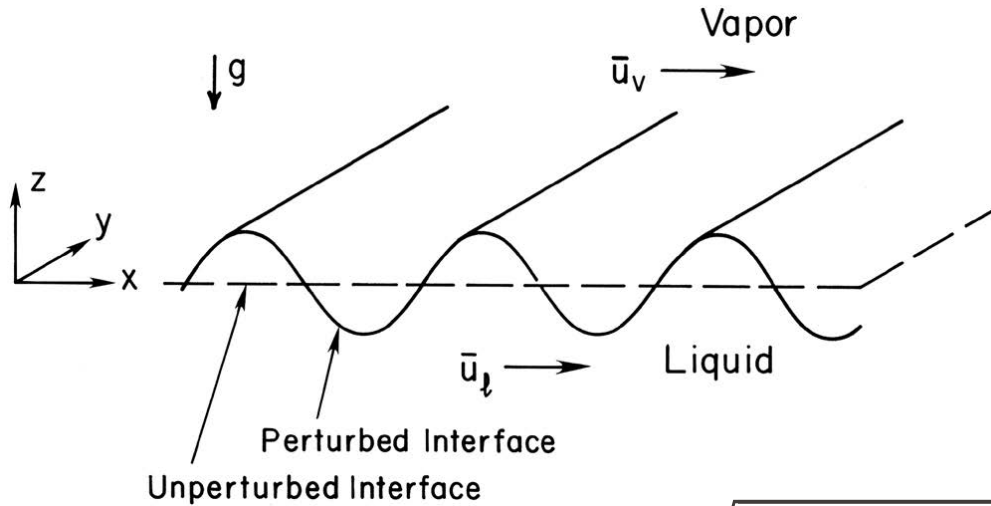
# Helmholtz Instability

$$a_v = \frac{\rho_v}{\alpha} (\beta A + i\alpha \bar{u}_v)^2 A$$

$$a_l = -\frac{\rho_l}{\alpha} (\beta A + i\alpha \bar{u}_l)^2 A$$

$$\hat{P}_v = a_v e^{-\alpha z} \quad \hat{P}_l = a_l e^{\alpha z}$$





$$\text{Perturbation } \delta(x, t = 0) = Ae^{i\alpha x}$$

$$\delta = Ae^{i\alpha x + \beta t}$$

$$w' = \hat{w}(z)e^{i\alpha x + \beta t}$$

$$p' = \hat{p}(z)e^{i\alpha x + \beta t}$$

$$\beta = \pm \frac{\sqrt{\alpha^2 \rho_v \rho_l (\bar{u}_v - \bar{u}_l)^2 - (\sigma \alpha^3 + \Delta \rho g \alpha)}}{\rho_v + \rho_l} - i\alpha \frac{\rho_l \bar{u}_l + \rho_v \bar{u}_v}{\rho_v + \rho_l}$$

The perturbation will cause a growing response if and only if  $\beta$  has a positive real part

Instability condition:

$$|\bar{u}_v - \bar{u}_l| > \sqrt{\frac{(\sigma \alpha + \frac{\Delta \rho g}{\alpha})(\rho_l + \rho_v)}{\rho_l \rho_v}}$$

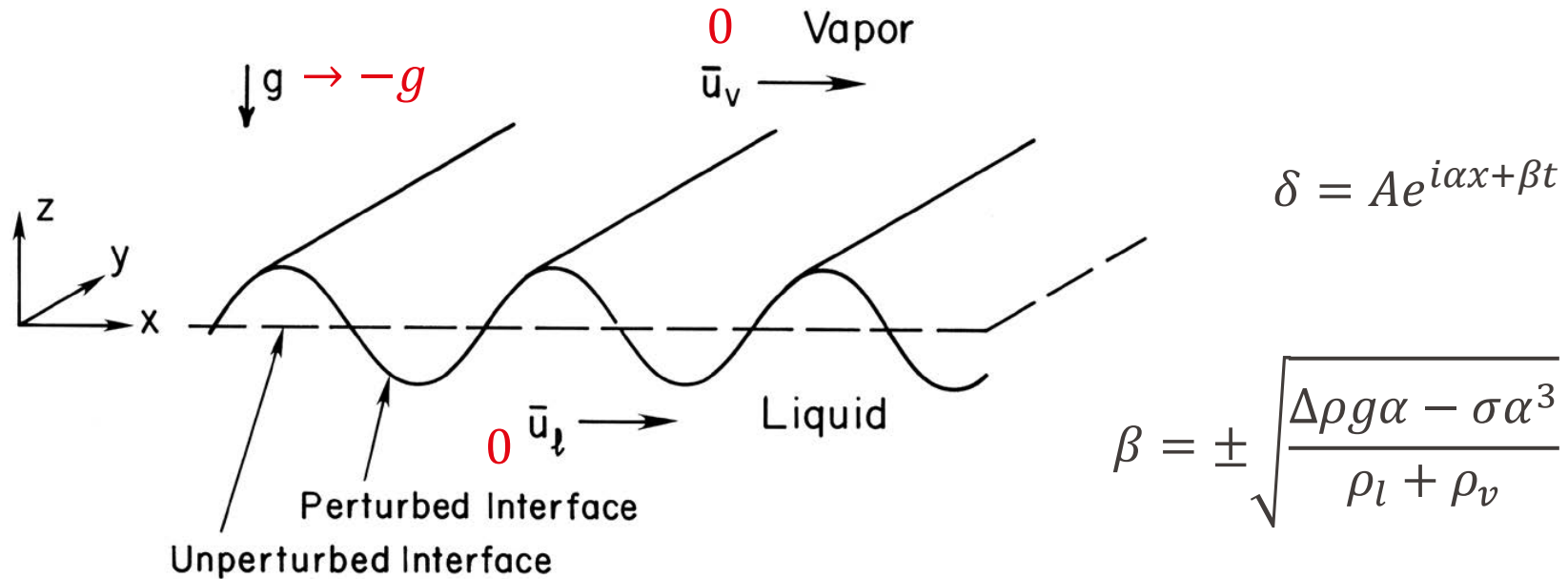
$\bar{u}_v - \bar{u}_l$  promotes instability while gravity and surface tension suppressing instability, we can adjust the value of  $g$  based on the orientation of the system.



# Helmholtz Instability



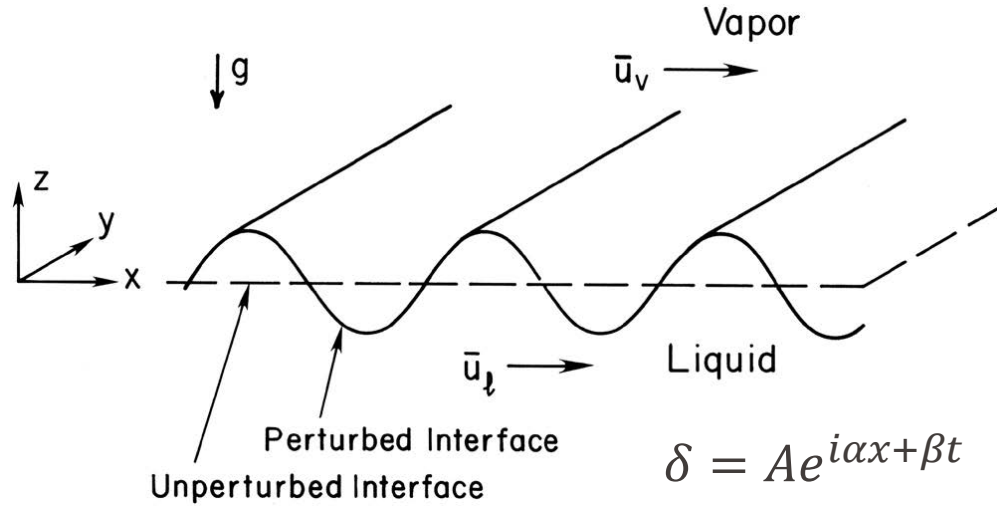
Facebook/ Rachel Gordon



The fastest growing perturbation ( $\alpha_{max}$ ) in this case can be found by setting  $\frac{d\beta}{d\alpha} = 0$

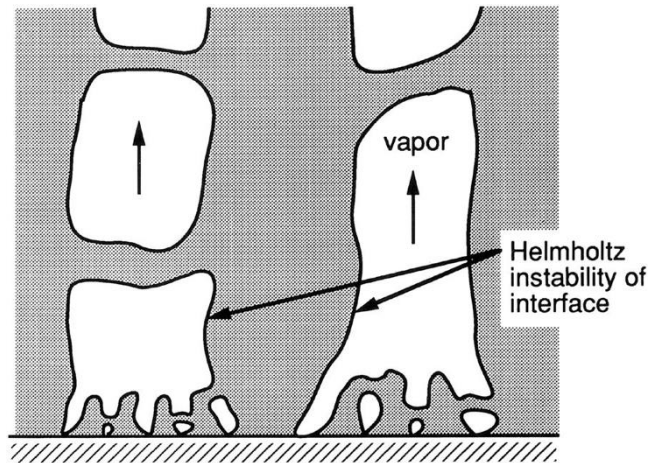
The corresponding most dangerous wavelength  $\lambda_D = \frac{2\pi}{\alpha_{max}} = 2\pi \sqrt{\frac{3\sigma}{\Delta\rho g}}$

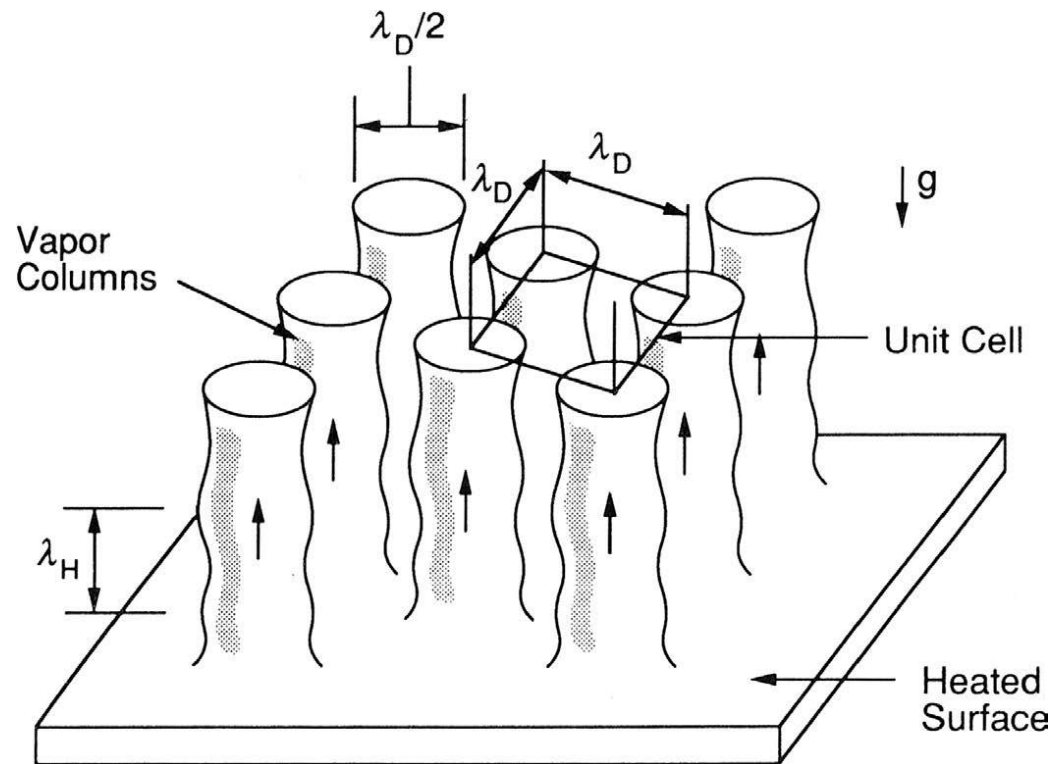
# How It's Related to Boiling



Helmholtz Instability

$$|\bar{u}_v - \bar{u}_l| > \sqrt{\frac{\left(\sigma\alpha + \frac{\Delta\rho g}{\alpha}\right) (\rho_l + \rho_v)}{\rho_l\rho_v}}$$





- CHF is reached when interface of vapor columns becomes Helmholtz unstable ( $\lambda_H$ )
- The pitch of the vapor columns coincides with the most dangerous wavelength in Taylor instability

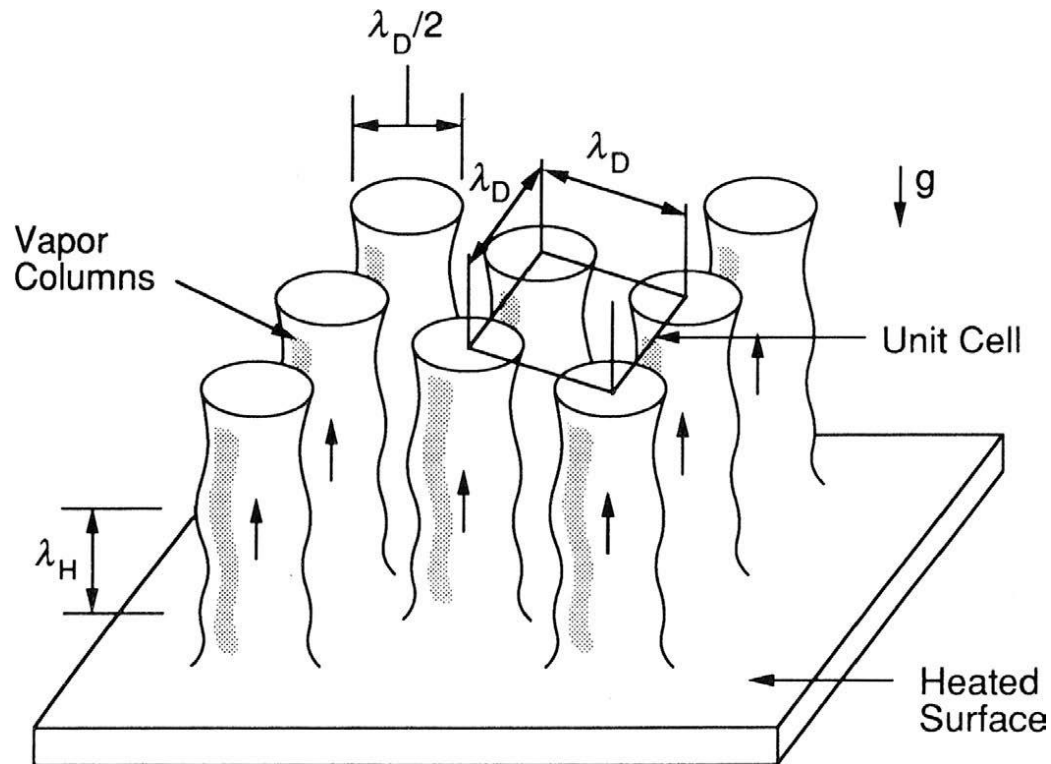
$$\lambda_D = 2\pi\sqrt{3\sigma/\Delta\rho g}$$

- The diameter of vapor column is  $\lambda_D/2$

$$\lambda_H = \lambda_D \Rightarrow u_c = \sqrt{\frac{2\pi\sigma(\rho_l + \rho_v)}{\rho_l\rho_v\lambda_H}} \approx \sqrt{\frac{2\pi\sigma}{\rho_v\lambda_D}}$$



$$u_c = \sqrt{\frac{2\pi\sigma}{\rho_v\lambda_D}} \quad \lambda_D = 2\pi \sqrt{\frac{3\sigma}{\Delta\rho g}}$$



$$u_c = \frac{q''_{max}}{\rho_v h_{lv}} \left( \frac{A_{surf}}{A_{col}} \right) = \frac{16 q''_{max}}{\pi \rho_v h_{lv}}$$

$$q''_{max} = 0.149 \rho_v h_{lv} \left( \frac{\sigma \Delta\rho g}{\rho_v^2} \right)^{1/4}$$

# Comments on Zuber's Model

- No way to accommodate effects from geometry and surface wettability
- No clear justification for the choice of vapor column diameter as  $\lambda_D/2$
- No visual observation of Helmholtz instability during boiling to date
- Still widely used as a reference model for all subsequent CHF models